



## Arsenic removal from water using a one-pot synthesized low-cost mesoporous Fe–Mn-modified biosorbent

JASMINA NIKIĆ<sup>1</sup>, MALCOLM WATSON<sup>1#</sup>, ALEKSANDRA TUBIĆ<sup>1#</sup>, MARIJANA KRAGULJ ISAKOVSKI<sup>1#</sup>, SNEŽANA MALETIĆ<sup>1#</sup>, EMILIJAN MOHORA<sup>2</sup> and JASMINA AGBABA<sup>1\*#</sup>

<sup>1</sup>University of Novi Sad, Faculty of Sciences, Department of Chemistry, Biochemistry and Environmental Protection, Trg Dositeja Obradovića 3, 21000 Novi Sad, Serbia and <sup>2</sup>Singidunum University, Faculty of applied ecology Futura, Požeška 83a, 11030 Beograd, Serbia

(Received 9 August, revised 8 November, accepted 13 November 2018)

**Abstract:** This paper investigates the removal of arsenic from water using an environmentally friendly modified biosorbent, chitosan coated with Fe–Mn binary oxide (Chit-FeMn), simply prepared with an one-pot low-cost procedure by simultaneous oxidation and coprecipitation. The sorbent was characterized by SEM, EDS, XRD, FTIR, BET specific surface area, and point of zero charge ( $\text{pH}_{\text{pzc}}$ ) measurements. The kinetic data fitted a pseudo-second order model for both As(III) and As(V), suggesting chemical adsorption on the sorbent surface and that intra-particle diffusion is not the only rate-limiting step during adsorption. The adsorption isotherms were best fit to the Freundlich model, and the non-monolayer adsorption model for arsenic on Chit-FeMn is therefore proposed. Below pH 9, the effect of pH on As(III) and As(V) removal by Chit-FeMn was insignificant, with As removals remaining above 85 %.  $\text{Cl}^-$  and  $\text{NO}_3^-$  had negligible influences on As(III) and As(V) removal, whereas  $\text{PO}_4^{3-}$ ,  $\text{SiO}_3^{2-}$ ,  $\text{CO}_3^{2-}$  and  $\text{SO}_4^{2-}$  were observed to compete with arsenic species for adsorption sites. The adsorbent was successfully applied to remove arsenic from real arsenic contaminated groundwater samples to below  $10 \mu\text{g L}^{-1}$  suggesting that Chit-FeMn is a promising candidate for the low cost removal of both As(V) and As(III) during drinking water treatment.

**Keywords:** adsorption; Chitosan; mechanism; competitive ions; groundwater.

### INTRODUCTION

Arsenic is considered as one of the most hazardous elements for living organisms and its presence in natural waters used as drinking water resources can cause serious public health problems. Arsenic contamination of groundwater has been reported in many countries around the world including Serbia.<sup>1</sup> It is well-

\*Corresponding author. E-mail: jasmina.agbaba@dh.uns.ac.rs

# Serbian Chemical Society member.

<https://doi.org/10.2298/JSC180809099N>

-known that long term consumption of arsenic polluted drinking water may cause cancer and other related diseases. Therefore, the World Health Organization (WHO) recommends a maximum allowable concentration (MAC) for arsenic in drinking water of  $10 \text{ } \mu\text{g L}^{-1}$ . This value has been endorsed by the European Union and other health organizations,<sup>2</sup> and is also applicable in the Republic of Serbia. However, many poorer countries still follow the earlier limit of  $50 \text{ } \mu\text{g L}^{-1}$ .<sup>3</sup>

Arsenic can be removed from water through oxidation, coagulation, adsorption, membrane technology and ion exchange technologies.<sup>4</sup> However, adsorption technologies are regarded as the most suitable techniques because the process is inexpensive, simple to operate, safe to handle and can be used at different scales ranging from household modules to community plants.<sup>5</sup> Different adsorbents are available for arsenic removal, however iron based adsorbents are still widely in use, because of their low cost and high affinity for arsenic. Moreover, in recent years iron oxides have been modified in order to get simultaneous oxidation of As(III) and adsorption of As(V).<sup>6–8</sup> In particular, Fe-Mn binary oxide materials have attracted a lot of attention as they combine the oxidation potential of  $\text{MnO}_2$  to convert As(III) to As(V) and the adsorption capacity of iron oxy-hydroxides, therefore providing simultaneous removal of both arsenic species.<sup>9–11</sup> However, most of these composite materials are in the form of powders and cannot be separated easily from aqueous solution which make the process difficult to apply. In addition, these fine powders cannot be used in columns due to their low hydraulic properties. Thus, in order to overcome such problems some authors have immobilized powdered Fe-Mn binary oxide onto different carriers. Chang *et al.*<sup>12</sup> incorporated Fe-Mn binary oxide onto diatomite (FMBO-diatomite) and the resultant sorbent showed high oxidation and adsorption ability for As(III). In other work, anion exchanger-supported Fe-Mn binary oxide was also shown to have great potential in As(III) removal from contaminated waters.<sup>13</sup> Rye *et al.*<sup>14</sup> reported the synthesis of granular activated carbon (GAC)-FeMn and used batch studies to investigate its potential for As(III) and As(V) removal.

Given the continued need to solve the problems with arsenic in drinking water sources as efficiently and economically as possible, the search for suitable adsorbents continues. In this work, we use the inexpensive, biodegradable and nontoxic biopolymer Chitosan as a carrier for Fe-Mn binary oxide and apply a simple one-pot method to prepare one such sorbent, Chit-FeMn, for arsenic removal from water. Batch experiments and FTIR analyses were applied to study the As(III) and As(V) adsorption mechanisms and capacities, and the influence of pH and the effect of competitive ions was also investigated. Finally, the local arsenic contaminated drinking water source was treated with Chit-FeMn to demonstrate its real life applicability.

## EXPERIMENTAL

*Materials*

Medium molecular weight chitosan was obtained from Sigma Aldrich. All chemicals and reagents used in this study were of analytical grade. Ferric sulphate ( $\text{FeSO}_4 \cdot 7\text{H}_2\text{O}$ , POCH Poland and S.A) and  $\text{KMnO}_4$  (Centrohem, Serbia) were used for the adsorbent preparation. Stock solutions of As(III) and As(V) of  $1 \text{ g L}^{-1}$  were prepared by dissolving  $\text{As}_2\text{O}_3$  and  $\text{As}_2\text{O}_5$  (obtained from Alfa Aesar, Thermo Fisher Scientific) in deionized water. Deionized water was ASTM type I, with a conductivity of less than  $0.056 \mu\text{S cm}^{-1}$ , a pH value of 7.3 and a  $\text{TOC} < 0.5 \text{ mg L}^{-1}$ .

*Adsorbent preparation*

The chitosan coated with Fe–Mn binary oxide was prepared in a single one-pot process, after modification of the method proposed by Zhang *et al.*<sup>15</sup> The key modification was in the application of chitosan as a carrier for the Fe–Mn binary oxide. 10 g of raw chitosan was added to 200 mL  $\text{KMnO}_4$  solution (0.015 M), prior to spraying 200 mL  $\text{FeSO}_4$  solution (0.045 M) into the  $\text{KMnO}_4$  solution while stirring vigorously. 5 M NaOH solution was added simultaneously to maintain the solution pH between pH 7.0 and 8.0. The suspension was continuously stirred for 1 h and stabilised at room temperature for 24 h. The suspension was then filtered, washed several times with fresh ultra-pure water to neutral pH and dried at 110°C for 4 h. The dried sorbent was crushed and stored in a desiccator before use.

*Adsorbent characterization*

Scanning electron microscopy (SEM) images were obtained by Hitachi TM3030 (Japan) and the elemental contents were analyzed by energy dispersive X-ray spectroscopy (EDS). X-ray diffraction (XRD) patterns were obtained by Philips PW automated X-ray powder diffractometer (USA). The specific surface area was obtained by nitrogen adsorption using the Brunauer–Emmett–Teller (BET) method and the mesopore and micropore volumes were determined using the BJH and t-test methods, using a Quantachrome autosorb TMiQ surface area analyzer. The point of zero charge ( $\text{pH}_{\text{pzc}}$ ) was determined according to the method described by Zhang *et al.*<sup>16</sup> Fourier transform infrared (FTIR) spectra of sorbents before and after arsenic adsorption were recorded by infrared spectrophotometer (FTIR Nexus 670, Thermo-nicolet, USA). Samples for FTIR determination were ground with spectral grade KBr in an agate mortar.

*Adsorption experiments*

Arsenic adsorption experiments were performed in 40 ml glass bottles containing 20 mL aqueous arsenic solution with adsorbent doses of  $0.5 \text{ g L}^{-1}$ . The solution pH was adjusted to  $7.0 \pm 0.2$  by adding 0.1 M  $\text{HNO}_3$  and/or NaOH; ionic strength was adjusted to 0.01 M with  $\text{NaNO}_3$ . The suspensions were shaken on an orbital shaker at 180 rpm at  $22 \pm 1^\circ\text{C}$ . Adsorption kinetics were studied with fixed As(III) or As(V) concentrations ( $0.5 \text{ mg L}^{-1}$ ) at specific time intervals: 0.25, 0.5, 0.75, 1, 1.5, 2, 4, 7, 9, 12, 18 and 24 h. Adsorption isotherms were obtained by varying the initial arsenic concentration ( $0.1$ – $1 \text{ mg L}^{-1}$ ). The effect of solution pH on the arsenic adsorption was investigated with a fixed As(III) or As(V) concentration ( $0.2 \text{ mg L}^{-1}$ ) by varying the initial pH from 3 to 11, and the release of Fe and Mn to the final solutions was also determined. To investigate the influence of coexisting anions such as phosphates, silicates, carbonates, sulphates, chlorides and nitrates, their corresponding sodium salts were introduced into the As(III)/As(V) solutions. Similarly, humic acid at concentrations of  $4$ – $12 \text{ mg C L}^{-1}$  was used to study the influence of natural organic matter (NOM). In all batch tests, after adsorption, the samples were filtered through a  $0.45 \mu\text{m}$  cellulose membrane filter and

the concentration of arsenic in the filtrate was determined by atomic absorption spectrophotometry (AAS).

#### *Chemical analysis*

pH measurements were carried out using an InoLab pH/ION 735 instrument. Arsenic concentrations were determined by Graphite Furnace Atomic Absorption Spectrophotometry (Perkin Elmer AAnalyst 700) according to EPA method 7010.<sup>17</sup> The practical quantitation limit (PQL) for the arsenic measurements was 0.5 µg L<sup>-1</sup>. Concentrations of iron and manganese were determined by flame atomic absorption spectrophotometry (Perkin Elmer AAnalyst 700) according to EPA method 7000b.<sup>18</sup> The PQL for Fe and Mn were 0.068 and 0.034 mg L<sup>-1</sup>, respectively. Dissolved organic carbon (DOC) contents were analysed after filtration through a 0.45 µm membrane filter on an Elementar LiquiTOCII, using Pt catalysed combustion at 850 °C to oxidize the carbon, in accordance with the standard method SPRS ISO 8245:2007.<sup>19</sup> The PQL of the method was 0.5 mg C L<sup>-1</sup>.

## RESULTS AND DISCUSSION

#### *Adsorbent characterization*

The SEM images of Chit and Chit-FeMn are given in Fig. S-1 of the Supplementary material to this paper. The surface of Chit-FeMn is covered with a large number of tiny Fe–Mn binary oxide aggregates, while the surface of Chit features relatively smooth larger granules. This indicates that Fe–Mn binary oxide was well dispersed on the chitosan surface, with the high degree of dispersion increasing the number of active sites on the chitosan which are available for adsorption. The elements present on the surface of Chit and Chit-FeMn were investigated by EDS analysis (Fig. S-2 of the Supplementary material). The chitosan surface consists of carbon, oxygen and nitrogen at 48.68, 29.34 and 21.98 mass %, respectively (Fig. S-2a). After modification, Fe and Mn are distributed on the surface and the oxygen content increased up to 41.88 %, establishing the presence of Fe–Mn binary oxide particles on the Chit surface. The analysis of the surface of Chit-FeMn revealed that the Fe and Mn is present at an Fe/Mn mole ratio of about 2.81, very close to the desired 3:1 ratio (Fig. S-2b).

The BET surface area of the synthesized Chit-FeMn was 1.99 m<sup>2</sup> g<sup>-1</sup>, almost 4 times higher than the non-impregnated Chit (0.58 m<sup>2</sup> g<sup>-1</sup>). This increase is in agreement with the SEM imagery where the finer structures on the surface of Chit-FeMn are readily apparent, and are similar to results obtained in other studies, whereby Gupta *et al.*<sup>20</sup> found that the BET surface area of chitosan coated with iron flakes (ICF) was 1.44 m<sup>2</sup> g<sup>-1</sup>, while the specific surface area of iron doped chitosan granules was found to be 1.48 m<sup>2</sup> g<sup>-1</sup>.<sup>21</sup> Furthermore, the mesopore volume of the Chit-FeMn sorbent was approximately 3 times higher (0.014 cm<sup>3</sup> g<sup>-1</sup>) than that of chitosan (0.005 cm<sup>3</sup> g<sup>-1</sup>), with the t-test method showing there are no micropores on Chit or Chit-FeMn. The results of the t-test method and the pore diameters of Chit and Chit-FeMn (15.5 and 14.2 nm) mean that according to the IUPAC classification<sup>22</sup> they may be considered as mesoporous

adsorbents (pore diameter in the range 2 to 50 nm). The points of zero charge of Chit and Chit-FeMn were pH 7.3 and 5.8, respectively.

X-ray diffraction patterns of Chit and Chit-FeMn, in the  $2\theta$  range of 10–80°, are given in Fig. S-3 of the Supplementary material.

The most significant difference observed between the two XRD patterns is the decreasing crystallinity of the compound after modification with Fe–Mn binary oxide. The XRD pattern of chitosan shows typical crystalline diffraction peaks at  $2\theta = 19.9^\circ$ <sup>23</sup> which weaken and become wider after modification indicating a non-crystalline nature and suggesting the Fe–Mn oxide particles are in a more stable amorphous form.<sup>15,16</sup> This is in agreement with Neto *et al.*<sup>24</sup> who reported that diffractograms of chitosan beads crosslinked with glutaraldehyde (Ch-CL) present a much lower crystallinity index when chitosan beads are used for immobilization of Fe(III) (Ch-FeCL).

#### Adsorption kinetics

The adsorption kinetics of As(III)/As(V) on Chit and Chit-FeMn are shown in Fig. 1a and b. It can be seen that the adsorption process is time dependent and can be divided into two steps. In the first step of the process, adsorption of As(III)/As(V) onto Chit and Chit-FeMn is fast due the large number of available sites on the sorbent surfaces. The adsorption rate is slower in the subsequent step because the concentration gradients reduce due to the accumulation of As ions on the surface. Equilibrium of As(III) and As(V) on Chit was reached after 12 h (720 min, Fig. 1a). In the case of adsorption of As(III) and As(V) on Chit-FeMn, equilibrium was reached after 18 h (1080 min, Fig. 1b).

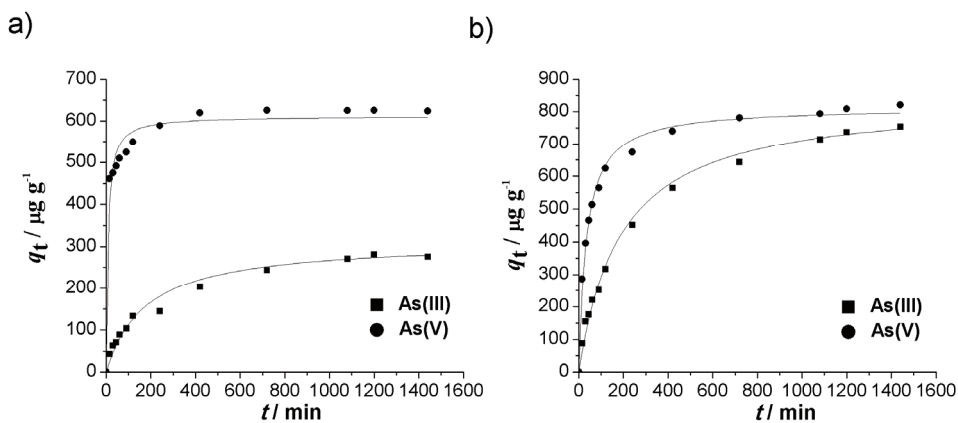


Fig. 1. Adsorption kinetics fitted with pseudo-first and pseudo-second order for As(III) and As(V) adsorption on: a) Chit and b) Chit-FeMn. Initial As(III)/As(V) concentration: 0.5 mg L<sup>-1</sup>, sorbent dose: 0.5 g L<sup>-1</sup>, pH 7.0±0.2.

In order to elucidate the adsorption mechanism, pseudo-first, pseudo-second order and Elovich models were initially used to fit the kinetic data.<sup>25</sup> Fit quality was determined using the coefficient of determination ( $R^2$ ) and the sum of the squared errors (SSE) to calculate the error deviation between the experimental and predicted data, for linear analysis (Table I).

TABLE I. Kinetic parameters for the adsorption of As(III) and As(V) onto Chit and Chit-FeMn adsorbents

| Model                             | Parameter                                      | Chit      |           | Chit-FeMn  |           |
|-----------------------------------|--|-----------|-----------|------------|-----------|
|                                   |  | As(III)   | As(V)     | As(III)    | As(V)     |
| Pseudo-first<br>order parameters  | $k_1 / \text{min}^{-1}$                        | 0.00169   | 0.00641   | 0.00389    | 0.00392   |
|                                   | $q_e / \mu\text{g g}^{-1}$                     | 239       | 124       | 807        | 457       |
|                                   | SSE  | 0.307     | 2.29      | 4.61       | 5.51      |
|                                   | $R^2$  | 0.9537    | 0.7456    | 0.8936     | 0.8766    |
| Pseudo-second<br>order parameters | $k_2 / \text{min}^{-1}$                        | 0.0000205 | 0.0000927 | 0.00000671 | 0.0000288 |
|                                   | $q_e / \mu\text{g g}^{-1}$                     | 308       | 725       | 840        | 833       |
|                                   | SSE  | 0.274     | 0.183     | 0.0137     | 0.00161   |
|                                   | $R^2$  | 0.9990    | 0.9642    | 0.9963     | 0.9996    |
| Elovich                           | $\alpha / \mu\text{g g}^{-1} \text{ min}^{-1}$ | 0.00160   | 0.113     | 0.000487   | 0.0122    |
|                                   | $\beta / \mu\text{g g}^{-1}$                   | 56        | 40.9      | 158        | 112       |
|                                   | SSE  | 2351      | 10853     | 2082       | 10243     |
|                                   | $R^2$  | 0.9710    | 0.9516    | 0.9827     | 0.9678    |

For SSE, a value closer to 0.0 indicates the model has a smaller random error component and that the fit is thus useful for prediction. In our work, lower SSE values and good coefficients of determination were observed for the second order kinetic model, for both As(III) and As(V) adsorption, indicating that the As(III) and As(V) sorption on Chit-FeMn may be due to chemisorptions.<sup>14</sup> Since the pseudo-second-order model well describes the reaction kinetics, it is limited in accuracy by considering the adsorption as a single, one-step binding process. However, the intraparticle diffusion model can provide a more comprehensive view of adsorption as a series of distinct steps. This model was therefore also employed to fit the kinetic data and the corresponding parameters of this model are present in Tables S-I of the Supplementary material. According to the model, if intraparticle diffusion is the rate-controlling step, the plot of  $q_t$  (sorption capacity at time  $t$ ) against  $t^{0.5}$  should be linear and pass through the origin. From Fig. 2, it can be clearly observed that none of the plots in their entirety pass through the origin, indicating that the mechanism of intraparticle diffusion is not the only limiting step of the adsorption process and that other interaction mechanisms must be acting simultaneously. Moreover, at each graph  $q_t$  vs.  $t^{0.5}$ , we observe two or three linear section with different gradients, which can be attributed to certain processes involved in the arsenic adsorption. The first segment (the initial steep part of the curves) corresponds to the rapid diffusion of arsenic through

the water matrix to the outer surface of the adsorbent (external diffusion). The second segment describes a gradual adsorption in which intraparticle diffusion limits the rate of the adsorption process. The third section, with the smallest slope, corresponds to the state of adsorption equilibrium, when the speed of the adsorption process is significantly slowed down due to the lower residual concentration of the arsenic. Thus, the rapid adsorption of arsenic from an aqueous solution corresponding to external diffusion and slower arsenic adsorption, caused by intraparticle diffusion, limits the entire adsorption process on the synthesized adsorbents. Similar observation was reported in study Neto *et al.*<sup>24</sup>

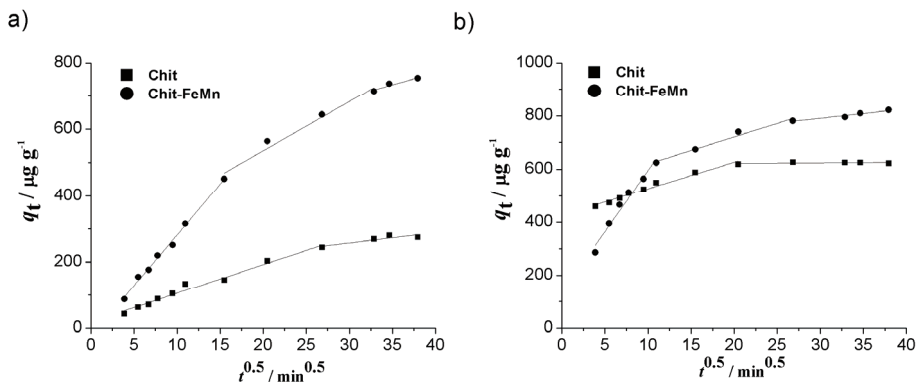


Fig. 2. Intraparticle mass transfer plot for: a) As(III) and b) As(V) adsorption on Chit and Chit-FeMn. Initial As concentration: 0.5 mg L<sup>-1</sup>, sorbent dose: 0.5 g L<sup>-1</sup>, pH 7.0±0.2.

#### Adsorption isotherms

In order to evaluate the adsorption capacities of Chit and Chit-FeMn for As(III) and As(V), the equilibrium data were fitted with the Freundlich (Fig. 3) and Langmuir models.<sup>26</sup>

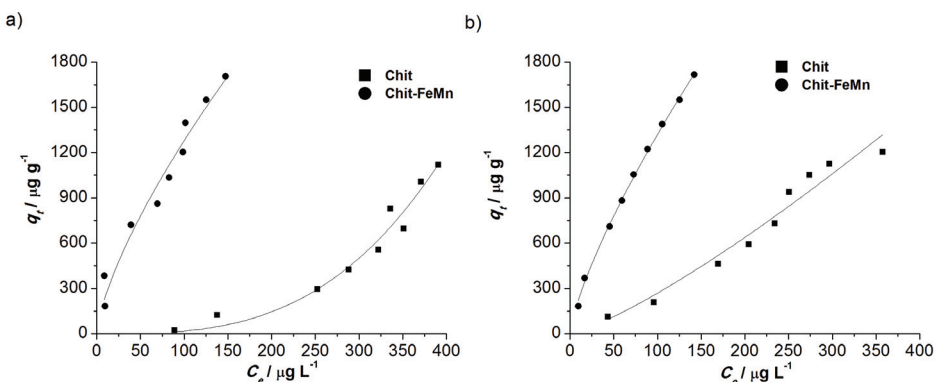


Fig. 3. Freundlich sorption isotherms for: a) As(III) and b) As(V) adsorption on Chit and Chit-FeMn. Initial As concentration: 0.1–1 mg L<sup>-1</sup>, sorbent dose: 0.5 g L<sup>-1</sup>, pH 7.0±0.2.

The values of the model parameters determined by linear regression analysis are presented in Table II.

TABLE II. Freundlich and Langmuir isotherm parameters for the adsorption of arsenic on Chit and Chit-FeMn

| Model      | Parameter   | Chit       |           | Chit-FeMn |           |
|------------|---|------------|-----------|-----------|-----------|
|            |   | As(III)    | As(V)     | As(III)   | As(V)     |
| Freundlich | $K_F / \mu\text{g g}^{-1} (\mu\text{g L}^{-1})^n$ | 0.000366   | 1.034     | 61.6      | 63.8      |
|            | $1/n$   | 2.499      | 1.21      | 0.655     | 0.798     |
|            | SSE   | 0.0926     | 0.0455    | 0.00689   | 0.00638   |
|            | $R^2$   | 0.9574     | 0.9499    | 0.9031    | 0.9912    |
| Langmuir   | $q_{\max} / \mu\text{g g}^{-1}$                   | 880        | 1225      | 3914      | 3893      |
|            | $K_L / \text{L g}^{-1}$                           | 0.00000542 | 0.0000571 | 0.0164    | 0.0187    |
|            | $R_L$   | 0.99-1.00  | 0.95-0.99 | 0.06-0.38 | 0.05-0.35 |
|            | SSE   | 1.221      | 1.013     | 0.0518    | 0.0211    |
|            |   | $R^2$      | 0.7234    | 0.8862    | 0.7094    |
|            |   |            |           |           | 0.9883    |

The Freundlich isotherm exhibited higher coefficient of determination ( $R^2$ ) and lower SSE values than the Langmuir model for both As(III) and As(V). The better fitting of the adsorption data to Freundlich isotherm (Fig. 3) indicated that the adsorption of both arsenic species preferably followed multilayer and heterogeneous adsorption process. The SEM images of Chit and Chit-FeMn showed the Chit and Chit-FeMn having rough structure development, therefore adsorbent was non-homogeneous. The  $K_F$  values from the Freundlich model show the much higher affinity of Chit-FeMn for both As(III) and As(V) in comparison with Chit. This confirms the fact that the impregnation of Fe–Mn binary oxide onto chitosan significantly increases the arsenic adsorption capacity of chitosan. The  $1/n$  values are less than 1, suggesting that the chemisorption of both arsenic species was the predominant adsorption process onto Chit-FeMn. In contrast, for the raw chitosan, the values of the Freundlich exponent  $1/n$  for As(III) and As(V) were 1.12 and 3.21, indicating that the physical adsorption is favoured.<sup>27</sup>

According to the Langmuir isotherm model, the maximum adsorption capacities,  $q_{\max}$ , for Chit were 0.88 and 1.22 mg g<sup>-1</sup> for As(III) and As(V), respectively, with much higher  $q_{\max}$  values observed (3.91 and 3.89 mg g<sup>-1</sup> for As(III) and As(V), respectively) for Chit-FeMn. The adsorption capacities reported in this current work are an improvement on the work of Gupta *et al.*<sup>20</sup> who found that the adsorption capacity of iron-doped chitosan granules (ICB) was 2.32 and 2.24 mg g<sup>-1</sup> for As(III) and As(V), respectively. Other authors have coated chitosan with a variety of different metals, including molybdate, titanium dioxide and iron(III)<sup>28-32</sup>. These authors also reported comparable adsorption capacities, ranging from 2.0 to 6.5 mg g<sup>-1</sup> for As(III) and from 0.43 to 2.1 mg g<sup>-1</sup> for As(V).

The values of  $R_L$ , an essential parameter of Langmuir isotherm, calculated at different initial concentrations of As(III) and As(V), were all between 0 and 1

(Table II), indicating that the adsorption onto Chit-FeMn is favourable for both As(III) and As(V).

#### *Effect of solution pH*

The pH of the aqueous solution, the most important parameter in adsorption studies, strongly affects the adsorption properties of iron-based sorbents. Hence, the influence of solution pH (from 3 to 11) on the removal of As(III) and As(V) by Chit-FeMn was investigated and the results are presented in Fig. 4.

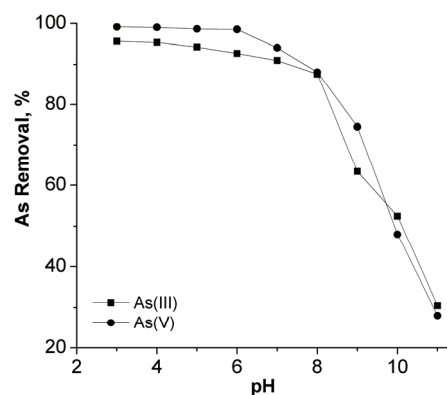


Fig. 4. Effect of initial solution pH on As(III) and As(V) removal by Chit-FeMn, initial As concentration:  $0.5 \text{ mg L}^{-1}$ , sorbent dose:  $0.5 \text{ g L}^{-1}$ .

The adsorption of arsenate was effective over the pH range 3–8, with removals not falling below 85 %. However, removal efficacy dropped upon further pH increases. A similar trend was observed for As(III) adsorption. The results can be explained by the point of zero charge ( $\text{pH}_{\text{pzc}}$ ) of the sorbent and the degree of protonation of arsenate in aqueous solution, which is a function of pH. The dissociation constants of aqueous arsenate are  $\text{pK}_1 = 2.3$ ,  $\text{pK}_2 = 6.8$  and  $\text{pK}_3 = 11.6$ , resulting in arsenate species varying from  $\text{H}_2\text{AsO}_3^-$ ,  $\text{HAsO}_3^{2-}$  and  $\text{AsO}_3^{3-}$  when the pH increases from acidic to alkaline (*i.e.*, pH 3–11 in this work). The  $\text{pH}_{\text{pzc}}$  of the synthesized Chit-FeMn was determined to be pH 5.8. It is well known that solid surfaces are positively charged at pH below their  $\text{pH}_{\text{pzc}}$  and negatively charged at pH above their  $\text{pH}_{\text{pzc}}$ .<sup>33</sup> Hence at  $\text{pH} < \text{pH}_{\text{pzc}}$  As(V) adsorption was promoted due to electrostatic attraction between the positively charged adsorbent surface and anionic As(V) species. However, the adsorption of As(V) decreased at  $\text{pH} > \text{pH}_{\text{pzc}}$  due to the electrostatic repulsion between the negatively charged adsorbent surface and negatively charged arsenic species. The removal of As(III) was very similar to As(V), remaining almost constant at better than 85 % removal in the pH range 3–8, then decreasing with further increases above pH 8. The  $\text{pK}_1$  value of  $\text{H}_3\text{AsO}_3$  is 9.2, indicating that As(III) exists as a neutral species at pH < 9.2 and as anions at pH > 9.2. The lower removal above pH 8 is therefore to be expected, given the electrostatic repulsion from the neg-

ative charge of the Chit-FeMn surface. Below pH 8, in the absence of favourable electrostatic interactions, the good removal of As(III) may be due to the oxidation reaction of As(III) to As(V) and sorption by iron oxide.<sup>33,34</sup> The oxidation of As(III) to As(V) by Mn oxides has been shown to be favourable at lower pH.<sup>13</sup> Furthermore, as discussed below, the oxidation of As(III) in the presence of manganese dioxide is accompanied by the reductive dissolution of MnO<sub>2</sub>, which leads to the release of Mn<sup>2+</sup>. These cations are then adsorbed on the sorbent surface, giving it a positive charge which facilitates the adsorption of arsenate oxy-anions in a neutral or alkaline environment.<sup>16,33,34</sup>

#### *Effect of competitive ions*

In general, ions such as phosphates, bicarbonates, silicates, sulphates, chlorides and nitrates can coexist with arsenic in groundwaters, and may interfere with arsenic removal *via* competitive binding or complexation. The effect of these anions on the adsorption of As(III) and As(V) by Chit-FeMn sorbents was examined at three different concentration levels (0.1, 0.5 and 1 mM) and the results are given in Fig. 5.

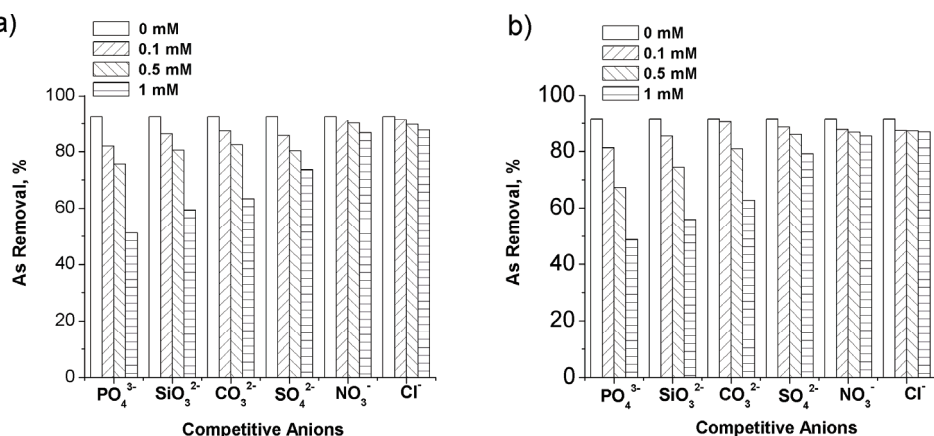


Fig. 5. Effect of coexisting anions on: a) As(III) and b) As(V) removal by Chit-FeMn; initial As concentration: 0.5 mg L<sup>-1</sup>, sorbent dose: 0.5 g L<sup>-1</sup>, pH 7.0±0.2.

The presence of chlorides and nitrates had only a slight influence on As(III) and As(V) removals. PO<sub>4</sub><sup>3-</sup> caused the greatest percentage decrease in arsenic removal at each concentration level, followed by SiO<sub>3</sub><sup>2-</sup>, CO<sub>3</sub><sup>2-</sup> and SO<sub>4</sub><sup>2-</sup>. Increasing the PO<sub>4</sub><sup>3-</sup> concentration from 0.1 to 1 mM reduced As(III) removals from 92 to 51 % (Fig. 5a). Similarly, the As(V) uptake by Chit-FeMn was reduced from 95 to 55 % (Fig. 5b). For SiO<sub>3</sub><sup>2-</sup>, an obvious decrease in arsenic removal was observed at 1 mM. As(III) and As(V) removals by Chit-FeMn decreased from 92 to 59 % and from 95 to 60 %, respectively. The arsenic, silicate and

phosphate oxyanions can all form inner-sphere complexes with the hydroxyl groups on the surface of adsorbents.<sup>35</sup> Thus the lower arsenic removals in the presence of phosphates and silicates can be attributed to the competition between  $\text{PO}_4^{3-}$  or  $\text{SiO}_3^{2-}$  and arsenic for adsorption sites. The decrease in As(III) and As(V) adsorption in the presence of  $\text{CO}_3^{2-}$  may result from the formation of arseno–carbonate complexes, including  $\text{As}(\text{CO}_3)^{2-}$ ,  $\text{As}(\text{CO}_3)(\text{OH})^{2-}$  and  $\text{AsCO}_3^+$ , which would prevent arsenic from forming inner-sphere complexes on the adsorbent surface.<sup>36</sup> The negative effect of the higher  $\text{SO}_4^{2-}$  concentration (1 mM) on As(III) and As(V) removal by Chit-FeMn may be attributed to the competition for active sites on the sorbent surface. In contrast, chloride and nitrate can only form outer-sphere complexes with ferric hydroxides, explaining the insignificant effect of these anions on arsenic removal. Hence, the order of interference for arsenite and arsenate adsorption on Chit-FeMn for the anions studied is phosphates > silicates > carbonates > sulphates > nitrates > chlorides.

#### *Effect of humic acid*

Natural organic matter, which is not only present everywhere in natural aquatic and soil environments but also highly reactive toward metals and surfaces, may interfere with the arsenic adsorption on the surfaces of minerals and therefore increase the mobility of arsenic. The effect of the presence of humic acid (4 to 12 mg DOC L<sup>-1</sup>) on arsenic sorption by the Chit-FeMn binary oxides was therefore investigated and the results are given in Fig. S-4 of the Supplementary material. Humic acid at the concentrations of up to 12 mg L<sup>-1</sup> had no obvious influence on As(V) removal. However, increasing the concentration of humic acid from 0 to 12 mg L<sup>-1</sup> decreased the percentage removal of As(III) by Chit-FeMn from 93 to 70 %.

#### *FTIR analysis*

A FTIR spectroscopic analysis was carried out to investigate the adsorption mechanism of As(III) and As(V) onto Chit-FeMn. The FTIR spectra of Chit-FeMn before and after sorption with As(III)/As(V) are shown in Fig. 6. All spectra exhibited bands at 3376 and 3434 cm<sup>-1</sup>, which is characteristic of the –OH and –NH stretching vibrations. Peak at 2920 cm<sup>-1</sup> could be attributed to –CH stretching vibration in –CH and –CH<sub>2</sub>. The peaks at 1634, 1540 and 1320 cm<sup>-1</sup> are attributed to stretching vibration (amide-I), N-H stretching vibration (amide-II) and the C–N stretching vibration, respectively. The peak at 1384 cm<sup>-1</sup> is due to symmetrical deformation of methyl (CH<sub>3</sub>) groups.<sup>37</sup> The peak at 1070 cm<sup>-1</sup> corresponds to the CO stretching vibration in –COH. After reaction with As(V), this peak disappears and a new peak appeared at 825 cm<sup>-1</sup>, corresponding to stretching vibration of As–O–Fe groups. This indicates that the As(V) is bound as a surface complex and not as a precipitated solid phase.<sup>38</sup> Similarly, after the adsorption of As(III), a small band at 825 cm<sup>-1</sup> appeared. This peak can be ascribed as an As–O stretching vib-

ration, which is characteristic of As(V) adsorption. Thus, this observation suggests that the part of the initial As(III) present was first oxidized to As(V) and then adsorbed onto the surface of the Fe–Mn oxides.<sup>39</sup>

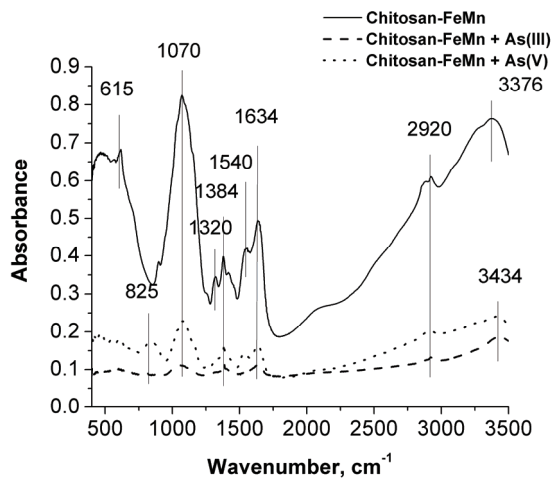


Fig. 6. FTIR spectra of Chit-FeMn before and after As(III) and As(V) adsorption.

In oxidative adsorption process for As(III) 1 M of MnO<sub>2</sub>(s) can oxidize 1 M of As(III), and subsequently releases 1 M of Mn<sup>2+</sup> into the aqueous phase.<sup>39</sup> Therefore, to further confirm the oxidation of As(III) on Chit-FeMn, the release pattern of soluble Mn<sup>2+</sup> from Chit-FeMn was determined after reaction with As(III) and As(V) at different solution pH. The concentration of dissolved iron was below the maximum allowed concentration (MAC) in all cases, indicating that the Chit-FeMn is stable under the conditions investigated (pH 3 to 11). In the case of As(V) adsorption, the release of Mn was also low (a maximum concentration of 0.098 mg L<sup>-1</sup> at pH 3). However, the significant amounts of Mn were released after As(III) adsorption, up to 1.82 mg L<sup>-1</sup> at pH 3. The greater release of manganese after As(III) adsorption can be attributed to the reductive dissolution of MnO<sub>2</sub> during As(III) oxidation.<sup>33,34</sup> Above pH 7, the release of Mn and Fe was not observed. Xu *et al.*<sup>40</sup> suggest that at this pH, the redox reaction which oxidizes As(III) does not progress far enough to generate excess Mn<sup>2+</sup>, with the As(III) adsorbing directly onto the adsorbent without oxidation.

The data presented above suggests that the mechanism of arsenic adsorption proceeds by the ligands exchange to form inner sphere complexes. The results for the pH dependence and the impact of ionic strength (nitrates investigated as competitive anions) show very little variation, which is suggestive of inner sphere complexes, according to Goldberg and Johnston<sup>41</sup> and Maliyekkal *et al.*<sup>42</sup> While Goldberg and Johnston<sup>41</sup> also reported that although arsenate forms inner sphere complexes with Fe oxides, arsenite can form both inner and outer sphere complexes, and the leaching of Mn from our sorbent during adsorption of As(III)

confirms the oxidation of As(III) prior to adsorption,<sup>33,34</sup> such that even during As(III) removal, the mechanism involves the adsorption of As(V). Finally, Kong *et al.*<sup>43</sup> investigated the adsorption of arsenic on a similar sorbent, nanoscale Fe–Mn binary oxides loaded on zeolite, and also proposed a ligand exchange mechanism forming inner-sphere complexes for both As(III) and As(V).

#### *Applicability of the adsorbent to naturally arsenic contaminated groundwater*

Groundwater used for water supply from Kikinda, Serbia (Table S-II of the Supplementary material), was treated with Chit-FeMn in order to investigate its potential to remove arsenic from naturally contaminated water sources. The initial As concentration in this water is  $35 \mu\text{g L}^{-1}$ , but it contains relatively high concentrations of natural organic matter, phosphate and sulphate, and has a high pH of 8.29. Despite the presence of these competitive anions and the unfavourable pH conditions, a Chit-FeMn sorbent dose of  $1.0 \text{ g L}^{-1}$  was sufficient to satisfy the WHO drinking water standards, indicating the strong suitability of this sorbent for full scale water treatment applications.

#### CONCLUSION

Chitosan coated with Fe–Mn binary oxide, an environmentally friendly biosorbent, was prepared in a single step process by the simultaneous redox and co-precipitation method. The kinetic study indicates that the adsorption of As(III) and As(V) on Chit-FeMn can be well described by the pseudo-second-order kinetic model. Maximal adsorption capacities of Chit-FeMn for As(III) and As(V) was 3.91 and  $3.89 \text{ mg g}^{-1}$ , respectively. The surface complexation is the major mechanism for As(III) and As(V) removal by Chit-FeMn. The removal efficiencies for both As(III) and As(V) were not significantly affected over a broad pH range (removals ranged from 99 to 88 % between pH 3 and 8), indicating that the sorbent is suitable for use in all typical groundwaters. Chit-FeMn also performed well with above 80 % removals for both As(III) and As(V) in the presence of less than  $8 \text{ mg DOC L}^{-1}$ . The presence of chlorides, nitrates, and sulphates had only a slight influence on As(III) and As(V) removal, whereas the presence of phosphates, silicates and carbonates significantly reduced the removal of both As(III) and As(V), especially at high concentrations. Results show that this modified biosorbent has the potential for application in the treatment of arsenic contaminated water, with investigations under dynamic conditions necessary in the future.

#### SUPPLEMENTARY MATERIAL

Additional data are available electronically at the pages of journal website: <http://www.shd.org.rs/JSCS/>, or from the corresponding author on request.

*Acknowledgement.* The authors gratefully acknowledge the support of the Ministry of Education, Science and Technological Development of the Republic of Serbia (Project No. III43005 and Project No. TR37004).

## ИЗВОД

УКЛАЊАЊЕ АРСЕНА ИЗ ВОДЕ ПРИМЕНОМ БИОСОРБЕНТА МОДИФИКОВАНОГ  
Fe–Mn БИНАРНИМ ОКСИДОМ

ЈАСМИНА НИКИЋ<sup>1</sup>, MALCOLM WATSON<sup>1</sup>, АЛЕКСАНДРА ТУБИЋ<sup>1</sup>, МАРИЈАНА КРАГУЉ ИСАКОВСКИ<sup>1</sup>,  
СНЕЖАНА МАЛЕТИЋ<sup>1</sup>, ЕМИЛИЈАН МОХОРА<sup>2</sup> и ЈАСМИНА АГБАБА<sup>1</sup>

<sup>1</sup>Универзитет у Новом Саду, Природно-математички факултет, Департман за хемију, биохемију и  
заштиту животне средине, Трг Доситеја Обрадовића 3, 21000 Нови Сад и <sup>2</sup>Универзитет Сингидунум,  
Факултет за применену еколођију Фуџура, Пожешка 83а, 11030 Београд

У раду је приказано уклањање арсена из воде применом биосорбента (Chitosan), који је модификован са Fe–Mn бинарним оксидом. Модификација Fe–Mn бинарним оксидом (Chit–FeMn) изведена је у једном степену, симултаним процесима оксидацije и копреципитације. Новосинтетисани сорбент је карактерисан различитим техникама, укључујући SEM/EDS, XRD, FTIR и BET анализу и одређивање тачке нултог наелектрисања. Сорбиционо понашање As(III) и As(V) на синтетисаном сорбенту испитивано је кинетичким и равнотежним експериментима, у шаржном систему. Установљено је да модел псевдо-другог реда најбоље описује кинетику адсорpcionог процеса оба облика арсена на Chit–FeMn, а да само унутарчестична дифузија није ограничавајући корак адсорpcionог процеса. Максимални адсорpcionи капацитети Chit–FeMn за As(III) и As(V) одређени Ленгмировим моделом износили су 3,91 и 3,89 mg g<sup>-1</sup>, редом. Промена pH вредности (од 3 до 8), није у већој мери утицала на степен уклањања As(III) и As(V) (>85 %), указујући да је сорбент прикладан за примену у подземним водама, без додатне корекције pH вредности. Међу испитиваним компетитирајућим јонима, фосфати, а затим силикати и карбонати, су испољили највећи инхибиторни утицај на сорпцију As(III) и As(V) на Chit–FeMn, док утицај хлорида, нитрата и сулфата није био од велиг значаја. Испитивања спроведена на реалним узорцима подземне воде указују на то да се применом модификованог биосорбента концентрација арсена може смањити испод максимално дозвољене концентрације од 10 µg L<sup>-1</sup>.

(Примљено 9. августа, ревидирано 8. новембра, прихваћено 13. новембра 2018)

## REFERENCES

1. D. Jovanovic, B. Jakovljevic, Z. Rasic-Milutinovic, K. Paunovic, G. Pekovic, T. Knezevic, *Environ. Res.* **111** (2011) 315 (<https://doi.org/10.1016/j.envres.2010.11.014>)
2. World Health Organisation (WHO), *Guidelines for drinking-water quality*, 4<sup>th</sup> ed., 2011
3. S. Shankar, U. Shanker, Shikha, *Sci World J.* **2014** (2014) 1 (<http://dx.doi.org/10.1155/2014/304524>)
4. N. N. Nicomel, K. Leus, K. Folens, P. V. De Voort, G. D. Laing, *Int. J. Environ. Res. Public Health* **13** (2016) 1 (<https://doi.org/10.3390/ijerph13010062>)
5. S. I. Siddiqui, S. A Chaudhry, *Process Saf. Environ. Prot.* **111** (2017) 592 (<https://doi.org/10.1016/j.psep.2017.08.009>)
6. L. Yu, X. Peng, F. Ni, J. Li, D. Wang, Z. Luan, *J. Hazard. Mater.* **246** (2013) 10 (<https://doi.org/10.1016/j.jhazmat.2012.12.007>)
7. G. Zhang, Z. Ren, X. Zhang, J. Chen, *Water Res.* **47** (2013) 4022 (<https://doi.org/10.1016/j.watres.2012.11.059>)
8. S.. Chaudhry, Z. Zaidi, S. I. Siddiqui, *J. Mol. Liq.* **229** (2017) 230 (<https://doi.org/10.1016/j.molliq.2016.12.048>)
9. Z. Jin, L. Zimo, L. Yu, F. Ruiqi, A. B. Shams, X. Xinhua, *RSC Adv.* **5** (2015) 67951 (<https://doi.org/10.1039/C5RA11601E>)

10. J. Nikić, J. Agbaba, M. Watson, S. Maletić, J. Molnar, B. Dalmacija, *Water Sci. Technol.: Water Supply* **16** (2016) 992 (<https://doi.org/10.2166/ws.2016.015>)
11. Y. Xiong, Q. Tong, W. Shan, Z. Xing, Y. Wang, S. Wen, Z. Lou, *App. Surf. Sci.* **416** (2017) 618 (<https://doi.org/10.1016/j.apsusc.2017.04.145>)
12. F. Chang, J. Qu, H. Liu, R. Liu, X. Zhao, *J. Colloid Interface Sci.* **338** (2009) 353 (<https://doi.org/10.1016/j.jcis.2009.06.049>)
13. X. Li, K. He, B. Pan, S. Zhang, L. Lu, W. Zhang, *Chem. Eng. J.* **193-194** (2012) 131 (<http://dx.doi.org/10.1016/j.cej.2012.04.036>)
14. S. R. Ryu, E. K. Jeon, J. S. Yang, K. Baek, *J. Taiwan Inst. Chem. Eng.* **72** (2017) 62 (<http://dx.doi.org/10.1016/j.jtice.2017.01.004>)
15. G.S Zhang, J.H. Qu, H.J. Liu, R.P. Liu, R.C. Wu, *Water Res.* **41** (2007) 1921 (<https://doi.org/10.1016/j.watres.2007.02.009>)
16. G. Zhang, H. Liu, J. Qu, W. Jefferson, *J. Colloid Interface Sci.* **366** (2012) 141 (<https://doi.org/10.1016/j.jcis.2011.09.058>)
17. US Environmental Protection Agency (USEPA), *Method 7010 Graphite Furnace Atomic Absorption Spectrophotometry, Revision 0*, 2007
18. US Environmental Protection Agency (USEPA), *Method 7000B Flame Atomic Absorption Spectrophotometry, Revision 2*, 2007
19. SRPS ISO 8245, *Guidelines for determination of total organic carbon (TOC) and dissolved organic carbon (DOC) in water*, 2007
20. A. Gupta, V. S Chauhan, P. N. Sankararamakrishnan, *Water Res.* **43** (2009) 3862 (<https://doi.org/10.1016/j.watres.2009.05.040>)
21. A. Gupta, N. Sankararamakrishnan, *Biores. Technol.* **101** (2010) 2173 (<https://doi.org/10.1016/j.biortech.2009.11.027>)
22. K. S. W. Sing, D. H. Evertt, R. A. W. Haul, L. R. A. Moscou, J. Pierotti, T. Rouquerol T. Siemieniewska, *Pure Appl. Chem.* **57** (1985) 603 (<http://dx.doi.org/10.1351/pac198557040603>)
23. B. Liu, X. Lv, D. Wang, Y. Xu, L. Zhang, Y. Li, *J. Appl. Polym. Sci.* **125** (2012) 246 (<https://doi.org/10.1002/app.35528>)
24. J.O.M. Neto, C.J. Bellato, J.L. Milagres, K.D. Pessoa, E.S. Alvarenga, *Water Braz. Chem. Soc.* **24** (2013) 121 (<http://dx.doi.org/10.1590/S0103-50532013000100017>)
25. L. Largitte, R. Pasquier, *Chem. Eng. Res. Des.* **109** (2016) 495 (<https://doi.org/10.1016/j.cherd.2016.02.006>)
26. N. Ayawei, A. N. Ebelegi, D. Wankasi, *J. Chem.* **2017** (2017) 1 (<https://doi.org/10.1155/2017/3039817>)
27. L. Lin, W. Qiu, D. Wang, Q. Huang, Z. Song, H. W. Chau, *Ecotoxicol. Environ. Saf.* **144** (2017) 514 (<http://dx.doi.org/10.1016/j.ecoenv.2017.06.063>)
28. D. Gang, B. Deng, L. Lin, *J. Hazard. Mater.* **182** (2010) 156 (<https://doi.org/10.1016/j.jhazmat.2010.06.008>)
29. C. Gerente, G. McKay, Y. Andrès, P. Le Cloreic, *Adsorption* **11** (2005) 859 (<https://doi.org/10.1007/s10450-005-6036-y>)
30. M. S Seyed Dorraji, A. Mirmohseni, F. Tasselli, A. Criscuoli, M. Carraro, S. Gross, A. Figoli, *J. Polym. Res.* **21** (2014) 1 (<https://doi.org/10.1007/s10965-014-0399-2>)
31. C. Y. Chen, T. H. Chang, J. T. Kuo, Y. F. Chen, Y. C. Chung, *Biores. Technol.* **99** (2008) 7487 (<https://doi.org/10.1016/j.biortech.2008.02.015>)
32. S. M. Miller, J. B. Zimmerman, *Water Res.* **44** (2010) 5722 (<https://doi.org/10.1016/j.watres.2010.05.045>)

33. D. Ocinski, I. J. Sobala, P. Mazur, J. Raczyk, E. K. Balawejder, *Chem. Eng. J.* **294** (2016) 210 (<http://dx.doi.org/10.1016/j.cej.2016.02.111>)
34. G. S. Zhang, J. H. Qu, H. J. Liu, R. P. Liu, G.T. Li, *Environ. Sci. Technol.* **41** (2007) 4613 (<https://doi.org/10.1021/es063010u>)
35. C. Shan, M. Tong, *Water Res.* **47** (2013) 3411 (<https://doi.org/10.1016/j.watres.2013.03.035>)
36. S. Zhang, H. Niu, Y. Cai, X. Zhao, Y. Shi, *Chem. Eng. J.* **158** (2010) 599 (<https://doi.org/10.1016/j.cej.2010.02.013>)
37. B. Mandal, S.K. Ray, *Mat. Sci. Eng., C* **44** (2014) 132 (<https://doi.org/10.1016/j.msec.2014.08.021>)
38. S. Kong, Y. Wang, H. Zhan, M. Liu, L. Liang, Q. Hu, *J. Geochem. Explor.* **144** (2014) 220 (<https://doi.org/10.1016/j.gexplo.2014.02.005>)
39. B. An, D. Zhao, *J. Hazard. Mater.* **211–212** (2012) 332 (<https://doi.org/10.1016/j.hazmat.2011.10.062>)
40. W. Xu, H. Xu, R. Wang, X. Liu, J. Zhao, J. Qu, *Chemosphere* **83** (2011) 1020 (<https://doi.org/10.1016/j.chemosphere.2011.01.066>)
41. S Goldberg, and C. T. Johnston, *J. Colloid Interface Sci.* **234** (2001) 204 (<https://doi.org/10.1006/jcis.2000.7295>)
42. S. M. Maliyekkala, L. Philip, T. Pradeep, *Chem. Eng. J.* **153** (2009) 101 (<https://doi.org/10.1016/j.cej.2009.06.026>)
43. S. Kong, Y. Wang, H. Zhan, S. Yuan, M. Yu, M. Liu, *Water Environ. Res.* **86** (2014) 147 (<https://doi.org/10.2175/106143013X13807328849170>).